

Cavity Self-Stabilization and Enhancement of Laser Gyroscopes by (Coupled) Optical Resonators

July 7, 2006

Abstract

We analyze the effect of a highly dispersive element placed inside a modulated optical cavity on the frequency and amplitude of the modulation to determine the conditions for cavity self-stabilization and enhanced gyroscopic sensitivity. Hence, we model cavity rotation or instability by an arbitrary AM/FM modulation, and the dispersive element as a phase and amplitude filter. We find that anomalous dispersion may be used to self-stabilize a laser cavity, provided the magnitude of the group index of refraction is smaller than the phase index of refraction in the cavity. The optimal stabilization is found to occur when the group index is zero. Group indices with magnitudes larger than the phase index (both normal and anomalous dispersion) are found to enhance the sensitivity of a laser gyroscope to rotation. Furthermore, our results indicate that atomic media, even coherent superpositions in multilevel atoms, are not useful for these applications, because the amplitude and phase filters work against one another, i.e., decreasing the modulation frequency increases its amplitude and vice-versa, with one exception: negative group indices whose magnitudes are larger than the phase index result in negative, but enhanced, beat frequencies. On the other hand, for optical resonators the dispersion reversal associated with critical coupling enables the amplitude and phase filters to work together under a greater variety of circumstances than for atomic media. We find that for single over-coupled resonators, or in the case of under-coupled coupled-resonator-induced absorption,

the absorption and normal dispersion on-resonance increase the contrast and frequency of the beat-note, respectively, resulting in a substantial enhancement of the gyroscopic response. Moreover, for cavity self-stabilization, we propose the use of a variety of coupled-resonator-induced transparency that is accompanied by anomalous dispersion.

1 Introduction

The additional phase shift acquired by an electromagnetic wave as a result of the motion of a medium, known as the Sagnac effect, accumulates each round-trip and is transformed into a frequency shift inside an optical cavity. The Doppler shift owing to the rotation of a ring laser, for example, is determined from the beat-frequency of two counter-propagating modes, which are made to interfere at a location outside the cavity. Ideally, for the measurement of motion, only the Sagnac effect contributes to the measured beat-note. There are, however, deleterious influences on the round-trip phase shift which can bias or obscure the measured beat frequency. Cavity instabilities, for example, produce random fluctuations in the round-trip phase-shift, and are known to limit the beat-note resolution to approximately 1Hz. Active electronic feedback techniques can increase this resolution by several orders-of-magnitude, but they suffer from inherent electronic noise and response time limitations. In addition, coupling between the counter-propagating modes as a result of (dissipative or conservative) backscattering and/or differential loss (or gain) can substantially reduce gyro sensitivities, or even result in a dead-band due to injection locking between the two modes.

In recent years there has been an interest in the development of highly dispersive materials whose resonant features can speed up, slow down, stop, store, or reverse the propagation of pulses of light [1], [2]. In particular, the use of coherent interactions in driven multilevel atoms or in multiple coupled resonators enables a large dispersion without the absorption typically associated with material resonances. Because of the practical difficulties associated with the use of electronic resonances in atomic gases, many researchers have focused on the development of analogous solid-state materials and integrated optical structures possessing similar characteristics. One key practical advantage to the use of optical resonators is that the coupling does not require external fields. Previously, we demonstrated that coherence effects such as electromagnetically-induced transparency (EIT),

electromagnetically-induced absorption (EIA), and gain-assisted superluminality (GAS) have analogies that can just as readily be implemented in systems of coupled optical resonators [15], [17], [16]. In this paper we discuss the use of elements with substantially modified group velocities within a laser cavity for the purpose of: (i) compensating undesirable phase shifts such as those due to cavity instabilities, and (ii) enhancing desirable phase shifts such as that due to rotation. The main point is that the dispersive element results in an additional phase-shift, whose size is dependent on the size of the effect to be compensated or enhanced.

The use of modified group velocities has been discussed for the enhancement of optical gyroscopes by several authors in recent years. Throughout this literature, however, conflicting conclusions are made, with some authors reporting an enhancement in sensitivity for normal dispersion [3, 4, 5, 6], and others for anomalous dispersion [7]. This is due, at least in part, to a confusion between the beat frequency and its derivative with respect to rotation. Shahriar pointed out that the enhancement predicted by many authors for an interferometric gyro containing a slow-light medium, applies only to relative rotation measurements, not to measurements of absolute rotation where the source and gyroscope are co-rotating and the Sagnac effect is independent of refractive index. The splitting of modes in a ring cavity, on the other hand, does depend on refractive index, and so it is possible to achieve a dispersion-related enhancement only in this case. In addition, Shahriar was the first to predict an enhancement for a fast-light medium, and found a critical anomalous dispersion (CAD) where the enhancement becomes nearly infinite at $n_g = 0$, limited only by higher-order dispersion. However, Shahriar's predictions of CAD, and those of other authors are in contrast with intracavity spectroscopy experiments on two-level atoms [9], which demonstrate that, within certain constraints, an enhancement occurs in the gyroscopic response for *both* normal and anomalous dispersion. Furthermore, a major shortcoming in all of these investigations is that they ignore the absorptive response of the medium, which acts as an amplitude filter.

Taken together, these inconsistencies and deficiencies emphasize the need for a more comprehensive understanding of the effect of such a highly dispersive medium on a rotating optical cavity, that agrees with experimental results. Toward this objective this end, we take a modulation spectroscopy approach. We derive the equations for the modulation spectroscopy of optical resonators incorporated into a laser cavity, and demonstrate that such a

resonator acts as an amplitude and phase filter, affecting (demodulating and shifting) the frequency components of the cavity instability or Doppler shift. Thus, we consider the modulation to be either deleterious (such as a cavity instability) or desirable (such as a rotation, index of refraction, or other thing to be sensed), and we derive the conditions under which the modulation may be enhanced or diminished.

2 Modulation Spectroscopy

Modulation spectroscopy[8] is a powerful technique commonly employed for determining the dispersive and absorptive characteristics of a medium. A weak low frequency amplitude or frequency modulation is incident on the medium to be examined. The phase delay and demodulation of the output are then related to the amount of advancement and attenuation, respectively, that a pulse would experience *if* it were to travel through that same medium. As we will discuss, the demodulation and phase shift are directly related to cavity self-stabilization and gyro enhancement.

Consider a mixed AM/FM modulation of carrier frequency $\omega_0 = ck_0$ and modulation frequency $\omega_m = ck_m$. The modulated electric field

$$\tilde{E}(z, t) = \tilde{\mathcal{E}}(z, t)e^{i(k_0 z - \omega_0 t + \varphi_0(z, t))} + c.c. \quad (1)$$

can be decomposed into its Fourier components,

$$\begin{aligned} \tilde{E}(z, t) &= \varepsilon_0(z, t)e^{i(k_0 z - \omega_0 t + \varphi_0(z, t))} \\ &+ \varepsilon_+(z, t)e^{i(k_+ z - \omega_+ t + \varphi_+(z, t))} \\ &+ \varepsilon_-(z, t)e^{i(k_- z - \omega_- t + \varphi_-(z, t))} + c.c., \end{aligned} \quad (2)$$

where $\omega_{\pm} = \omega_0 \pm \omega_m = ck_{\pm}$, frequencies are indicated by subscripts, and quantities that are modulated or rapidly-varying in z or t are denoted with a tilde. Alternatively, the field can be decomposed into its carrier and modulated components,

$$\tilde{\mathcal{E}}(z, t) = \varepsilon_0(z, t) + \tilde{\mathcal{E}}_m(z, t), \quad (3)$$

where the modulated field is

$$\begin{aligned} \tilde{\mathcal{E}}_m(z, t) &= \left[\varepsilon_+(z, t)e^{i(k_m z - \omega_m t + \varphi_+(z, t))} \right. \\ &\left. + \varepsilon_-(z, t)e^{-i(k_m z - \omega_m t - \varphi_-(z, t))} \right] e^{-i\varphi_0(z, t)}. \end{aligned} \quad (4)$$

The modulation may be further decomposed into its AM/FM components,

$$\tilde{\mathcal{E}}_m(z, t) = \mathcal{E}^{AM}(z, t) + i\mathcal{E}^{FM}(z, t). \quad (5)$$

In writing Eq. (2) we have assumed that any FM component of the signal is sufficiently weak that there are not more than two sidebands in the frequency spectrum. The AM component is purely real regardless of the strength of the modulation, but the FM component is purely imaginary only within this approximation. When the sidebands are of equal amplitude, it is common to define a relative modulation index $M(z, t) = \varepsilon_+(z, t)/\varepsilon_0(z, t)$. Note that each frequency has its own slowly-varying amplitude and phase, which determines the relative modulation index, $M(z, t)$, as well as the AM/FM signal mixture. For a pure AM signal the two sidebands have equal amplitudes and are in-phase, whereas for a pure FM signal they have equal amplitudes but are anti-phased. We will consider the cases of an FM signal with $M \ll 1$, and an AM signal with $M \gg 1$.

Depending on the experimental configuration of interest, it is convenient to incorporate the sideband phase, $\varphi_{\pm}(z, t)$, into either the spatial or the temporal modulation frequency, i.e., we recast Eq. (4) in terms of either the spatial or temporal heterodyne beat-frequency. Furthermore, we are often not concerned with global phase factors and losses, so we divide the modulated field by that of the carrier to obtain the relative modulation

$$\begin{aligned} \tilde{\mathcal{M}}(z, t) &= \frac{\tilde{\mathcal{E}}_m(z, t)}{\varepsilon_0(z, t)} \\ &= \mathcal{M}(z, t)e^{i\varphi_m(z, t)} \left[\cos(\psi)e^{i(k_m z - \omega_b t)} + \sin(\psi)e^{-i(k_m z - \omega_b t)} \right] \\ &= \mathcal{M}(z, t)e^{i\varphi_m(z, t)} \left[\cos(\psi)e^{i(k_b z - \omega_m t)} + \sin(\psi)e^{-i(k_b z - \omega_m t)} \right], \quad (6) \end{aligned}$$

where $\omega_b(z, t)t = \omega_m t - \theta(z, t)/2$ is the temporal beat frequency, $k_b(z, t)z = k_m z + \theta(z, t)/2$ is the spatial beat frequency, $\theta(z, t) = \varphi_+(z, t) - \varphi_-(z, t)$ is the phase difference, and $\tan \psi(z, t) = \mathcal{E}_-(z, t)/\mathcal{E}_+(z, t)$ is the amplitude ratio of the interfering sidebands, respectively. The slowly-varying relative modulation amplitude and phase (with respect to the carrier) are $\mathcal{M}(z, t) = \mathcal{E}_m(z, t)/\varepsilon_0(z, t) = [\varepsilon_+(z, t)^2 + \varepsilon_-(z, t)^2]^{1/2}/\varepsilon_0(z, t)$ and $\varphi_m(z, t) = [\varphi_+(z, t) + \varphi_-(z, t)]/2 - \varphi_0(z, t) = \theta(z, t)/2 + \varphi_-(z, t) - \varphi_0(z, t)$, respectively. Note that the amplitude $\mathcal{M}(z, t)$ becomes simply $\sqrt{2}M(z, t)$ when the sidebands have equal amplitudes. We shall primarily be concerned with temporal,

rather than spatial, beat-frequencies, in accordance with our aim of studying perturbed laser cavities.

A parametric plot of Eq. (6) traces out, at the frequency ω_m , an ellipse of eccentricity $\sqrt{2 \sin \psi \cos \psi} / (\cos \psi + \sin \psi)$ and tilt angle $\theta/2$ with respect to the horizontal axis, as shown in Fig. 2c. The vertical(horizontal) axis determines the FM (AM) component of the modulation. The special case of a single sideband ($\psi = 0$ or $\pi/2$) is simply represented by a circle (with opposite rotation for the two different sidebands). Equal amplitude sidebands $\psi = \pi/4$ are represented by a straight line, with $\theta = 0$ for the pure AM case and $\theta = \pi$ for the pure FM case. In general, the modulation ellipse evolves in size and shape as a result of propagation through a medium or interaction with a structure, until a steady-state is reached. Neglecting terms of the order of M^2 , the intensity of the modulated signal is

$$I(z, t) = \frac{c}{4\pi} \langle \tilde{E}(z, t)^2 \rangle \approx \frac{c}{2\pi} [\varepsilon_0(z, t)^2 + 2\varepsilon_0(z, t)\mathcal{E}^{AM}(z, t)]. \quad (7)$$

The FM signal component does not contribute to the intensity, except insofar as the evolution of the modulation ellipse transforms it to an AM signal.

The modulation in the frequency domain (ignoring negative frequencies) is obtained from the temporal Fourier transform of Eq. (2),

$$\begin{aligned} \tilde{E}(\omega, z) &= \varepsilon_0(z) \delta(\omega - \omega_0) e^{i(k_0 z + \varphi_0(z))} \\ &+ \varepsilon_+(z) \delta(\omega - \omega_+) e^{i(k_+ z + \varphi_+(z))} \\ &+ \varepsilon_-(z) \delta(\omega - \omega_-) e^{i(k_- z + \varphi_-(z))}. \end{aligned} \quad (8)$$

In performing the Fourier transform we have assumed that the variation in t is sufficiently slow in comparison with the time-scale of interest (the time between structures) that we can drop the time-dependencies in the slowly-varying quantities, and obtain perfect delta-functions in frequency.

Now, let us determine the effect of a sequence of (coupled) resonators on the modulation. The response function for one such (coupled) resonator structure is

$$\tau(\omega) = |\tau(\omega)| e^{i\tilde{\Phi}(\omega)} = e^{i\tilde{\Phi}(\omega)}, \quad (9)$$

where $\tilde{\Phi}(\omega) = \Phi(\omega) + iA(\omega)/2$ is the complex effective phase-shift, $\Phi(\omega)$ is the effective phase-shift, and $A(\omega) = -2 \ln |\tau(\omega)|$ is the effective loss coefficient of the resonator structure, respectively. Where there is the possibility of confusion, capitalized letters will be used throughout this discussion to distinguish effective versions of material quantities from their non-effective

counterparts. For p passes across the structure, the response function is modified,

$$\tau(\omega, z) = e^{ip(\tilde{\Phi}(\omega) + \tilde{\varphi}(z))}. \quad (10)$$

where $\tilde{\varphi}(z) = \varphi(z) + i\alpha(z)/2$ is the contribution to the complex phase shift due to the intervening material between the resonator structures, $\phi(z)$ is single-pass phase-shift, and $\alpha(z)$ is the net dimensionless loss (or gain) coefficient. We assume that the frequency dependence of $\tilde{\varphi}(z)$ is weak in comparison with that of $\tilde{\Phi}(\omega)$. Hence, the factor $\tilde{\varphi}$ is simply a global complex phase shift, whose real part, $\varphi(z)$, is a global phase factor that can be neglected, and whose imaginary part, $\alpha(z)$, causes an overall attenuation (or gain). We lump all forms of gain or loss into $\alpha(z)$. In the case of a laser, under steady-state conditions, the total loss would be compensated by the saturated gain at the lasing wavelength. We shall consider two cases: (i) a laser operating at ω_0 with noise components modeled by weak ($M \ll 1$) FM side-band frequencies (Fig. 2a), and (ii) a rotating (or otherwise perturbed) laser gyro, whose counter-propagating frequencies of ω_+ and ω_- are modeled by strong ($M \gg 1$) AM side-bands that interfere with one another resulting in a beat-note, and where residual backscattering is modeled by a weak carrier frequency (Fig. 2b). Hence, the threshold conditions are $A_0 + \alpha = 0$ and $A_{\pm} + \alpha = 0$, for cases (i) and (ii), respectively, i.e., the presence of the structure modifies the lasing threshold. We assume that the saturated gain line is much broader than the spectrum of the resonator structure, which in turn is much broader than the frequency components of the modulation, such that the effect of the gain medium can be lumped into $\tilde{\varphi}(z)$. This assumption is good provided the laser cavity is much larger than the resonators.

The transmitted electric-field in the frequency domain is given by

$$\tilde{E}^t(\omega, z) = \tilde{E}^i(\omega, z)\tau(\omega, z). \quad (11)$$

For the input electric field, $\tilde{E}^i(\omega, z)$, we use Eq. (8) but first drop the z -dependencies in the slowly-varying amplitudes and phases, since we explicitly account for it by use of the transfer function. Neglecting the global phase factor, $\varphi(z)$, we obtain

$$\begin{aligned} \tilde{E}^i(\omega, z) = & \left[\varepsilon_0 \delta(\omega - \omega_0) e^{i(k_0 z + p\tilde{\Phi}_0 + \varphi_0)} \right. \\ & + \varepsilon_+ \delta(\omega - \omega_+) e^{i(k_+ z + p\tilde{\Phi}_+ + \varphi_+)} \\ & \left. + \varepsilon_- \delta(\omega - \omega_-) e^{i(k_- z + p\tilde{\Phi}_- + \varphi_-)} \right] e^{-p\alpha(z)/2}. \end{aligned} \quad (12)$$

Hence the (coupled) resonator sequence acts as an amplitude and phase filter on these three frequencies. The effect of this filter is entirely described by the complex effective phase-shift $\tilde{\Phi}$. The real-valued quantities A and Φ , describe the amplitude and phase filters, respectively. Simply considering the effect of the amplitude filter, it is clear from this expression that a single non-amplifying resonator (or non-inverted two-level atom) would absorb more of the carrier than the side bands, thereby increasing the relative modulation amplitude. The opposite is true of amplifying single resonators or inverted two-level atoms, and of coupled structures or three-level atoms that demonstrate induced transparency. Next we will examine the effect of the phase filter.

We take the inverse Fourier transform back to the time domain to obtain the transmitted electric field

$$\tilde{E}^t(z, t) = \tilde{\mathcal{E}}^t(z, t)e^{i(k_0 z - \omega_0 t + \varphi_0 + p\Phi_0)} + c.c. \quad (13)$$

and, as in Eq. (3), factor out the rapid variation and separate the result into a carrier signal,

$$\varepsilon_0^t(z) = \varepsilon_0 e^{-p(\alpha(z) + A_0)/2}, \quad (14)$$

and a modulation,

$$\begin{aligned} \tilde{\mathcal{E}}_m^t(z, t) = & \left[\varepsilon_+ e^{i(k_m z - \omega_m t + \varphi_+)} e^{ip\tilde{\Phi}_+} \right. \\ & \left. + \varepsilon_- e^{-i(k_m z - \omega_m t - \varphi_-)} e^{ip\tilde{\Phi}_-} \right] e^{-(\varphi_0 + p\Phi_0)} e^{-p\alpha/2}, \end{aligned} \quad (15)$$

where $\tilde{\mathcal{E}}^t(z, t) = \varepsilon_0^t(z) + \tilde{\mathcal{E}}_m^t(z, t)$. Note that Eq. (15) can be obtained directly from Eq. (4), if we ignore the slowly-varying dependence on t , make the transformations,

$$\begin{aligned} \varphi_{0,\pm}(z) & \rightarrow \varphi_{0,\pm} + p(\varphi(z) + \Phi_{0,\pm}) \\ \varepsilon_{0,\pm}(z) & \rightarrow \varepsilon_{0,\pm} \exp[-p(\alpha(z) + A_{0,\pm})], \end{aligned} \quad (16)$$

and ignore the global phase factor $\varphi(z)$. Because $\tilde{\varphi}(z)$ is a global complex phase factor, it does not contribute to the beat-frequency, nor to the relative evolution of the modulation ellipse, i.e., it does not change $M(z, t)$, nor does it change the AM/FM signal mixture. Thus, in the absence of the structures, Eq. (6) suffices to describe the modulation, provided we drop all slowly-varying dependencies. Our assumption is, therefore, that the relative

modulation does not evolve, or evolves only weakly, in the absence of the structures.

In the presence of the resonator structures, on the other hand, the strong frequency-dependence of $\tilde{\Phi}(\omega)$ modifies the beat-frequency, and causes the modulation ellipse, the relative modulation index, and the AM/FM signal mixture to evolve. We rewrite Eq. (15) in form similar to that of Eq. (6), i.e.,

$$\begin{aligned}\tilde{\mathcal{M}}^t(z, t) &= \mathcal{M}(z)e^{i\Phi_m} \left[\cos(\psi)e^{i(k_m z - \Omega_b t)} + \sin(\psi)e^{-i(k_m z - \Omega_b t)} \right] \\ &= \mathcal{M}(z)e^{i\Phi_m} \left[\cos(\psi)e^{i(K_b z - \omega_m t)} + \sin(\psi)e^{-i(K_b z - \omega_m t)} \right] \quad (17)\end{aligned}$$

where $\Omega_b t = \omega_m t - \Theta/2$ is the effective temporal beat frequency, $K_b z = k_m z + \Theta/2$ is the spatial beat frequency, $\theta = \varphi_+ - \varphi_-$ is the initial phase difference, $\Theta = \theta + p(\Phi_+ - \Phi_-)$ is the effective phase difference, and $\tan \psi = \mathcal{E}_- \exp(-pA_-/2)/\mathcal{E}_+ \exp(-pA_+/2)$ is the amplitude ratio of the interfering sidebands, respectively. The relative modulation amplitude and phase are $\mathcal{M}(z) = \mathcal{E}_m(z)/\mathcal{E}_0(z) = [\mathcal{E}_+^2 \exp(-pA_+) + \mathcal{E}_-^2 \exp(-pA_-)]^{1/2} \exp[-p\alpha(z)/2]/\mathcal{E}_0 \exp(-pA_0/2)$, and $\Phi_m = [(\varphi_+ + \varphi_-) + p(\Phi_+ + \Phi_-)]/2 - (\varphi_0 + p\Phi_0) = \Theta/2 + (\varphi_- + p\Phi_-) - (\varphi_0 + p\Phi_0)$, respectively. Alternatively, the amplitude variation of $\mathcal{E}_m(z)$ can be incorporated into the beat-frequency while that of $\mathcal{E}_0(z)$ is incorporated into Φ_m , i.e., Eq. (17) can be cast in terms of complex quantities

$$\begin{aligned}\tilde{\mathcal{M}}^t(z, t) &= \mathcal{M}e^{i\tilde{\Phi}_m(z)} \left[\cos(\psi)e^{i[k_m z - \tilde{\Omega}_b(z)t]} + \sin(\psi)e^{-i[k_m z - \tilde{\Omega}_b(z)t]} \right] \\ &= \mathcal{M}e^{i\tilde{\Phi}_m(z)} \left[\cos(\psi)e^{i[\tilde{K}_b(z)z - \omega_m t]} + \sin(\psi)e^{-i[\tilde{K}_b(z)z - \omega_m t]} \right] \quad (18)\end{aligned}$$

where $\tilde{\Omega}_b(z)t = \omega_m t - \tilde{\Theta}(z)/2 = \Omega_b t - ipA_b/2$ and $\tilde{K}_b(z)z = k_m z + \tilde{\Theta}(z)/2 = K_b z + ipA_b/2$ are the complex effective beat frequencies, $A_b = \alpha + (A_+ + A_-)/2$ is the total average effective loss, $\tilde{\Theta}(z) = \theta + p[\tilde{\Phi}_+(z) - \tilde{\Phi}_-^*(z)] = \Theta + iA_b$ is the complex effective phase difference, and $\tan \psi = \mathcal{E}_-/\mathcal{E}_+$ is the amplitude ratio, respectively. The relative modulation amplitude and phase are $\mathcal{M} = \mathcal{E}_m/\mathcal{E}_0 = [\mathcal{E}_+^2 + \mathcal{E}_-^2]^{1/2}/\mathcal{E}_0$, and $\tilde{\Phi}_m(z) = ([\varphi_+ + \varphi_-] + p[\tilde{\Phi}_+(z) + \tilde{\Phi}_-^*(z)])/2 - [\varphi_0 + p\tilde{\Phi}_0(z)] = \tilde{\Theta}(z)/2 + [\varphi_- + p\tilde{\Phi}_-^*(z)] - [\varphi_0 + p\tilde{\Phi}_0(z)]$, respectively. For clarity, amplitude variations of effective quantities with z are explicitly indicated, but phase variations are not, i.e., the dependency of Ω_b on z is implicit.

Notice that when the carrier frequency is on-resonance with the structure the attenuation of the side-bands is balanced, i.e., $A_+ = A_-$. In this case,

when $p(\Phi_+ - \Phi_-) = 2q\pi$, where q is an integer, the mixture of the AM/FM signal shown in Eq. (5) is not altered by the structure (though a phase-shift and demodulation occur, i.e., there is a change in beat-frequency and relative modulation). On the other hand, when the carrier frequency is off-resonance there is always a change in the AM/FM signal mixture since $A_+ \neq A_-$. Again, only the AM part of the output signal contributes to the modulated intensity. However, the presence of the resonators can transform a purely FM input to an AM output signal, thereby affecting the output intensity, which we obtain from Eq. (7) as

$$I^t(z, t) = I_0^t \left[1 + \frac{2}{\mathcal{E}_0 |\tau_0|^p} \tilde{\mathcal{E}}^{AM}(z, t) \right] \quad (19)$$

where $I_0^t = (c/2\pi) \mathcal{E}_0^2 e^{-p(\alpha + A_0)}$ is the transmitted intensity of the carrier, and

$$\begin{aligned} \tilde{\mathcal{E}}^{AM}(z, t) = & \mathcal{E}_+ |\tau_+|^p \cos[(\Phi_m + \Theta/2) + (k_m z - \omega_m t)] \\ & + \mathcal{E}_- |\tau_-|^p \cos[(\Phi_m - \Theta/2) - (k_m z - \omega_m t)], \end{aligned} \quad (20)$$

is the transmitted AM field obtained from Eq. (17). This output signal represents the heterodyne interference of the carrier with the two sidebands, and can be separated into components that are in-phase and in-quadrature with the modulation, i.e.,

$$I^t(z, t) = I_0^t [1 + \beta \cos(k_m z - \omega_m t) + \gamma \sin(k_m z - \omega_m t)], \quad (21)$$

where

$$\begin{aligned} \beta &= 2 \left[\frac{\mathcal{E}_- |\tau_-|^p \cos(\Phi_m - \Theta/2) + \mathcal{E}_+ |\tau_+|^p \cos(\Phi_m + \Theta/2)}{\mathcal{E}_0 |\tau_0|^p} \right] \\ \gamma &= 2 \left[\frac{\mathcal{E}_- |\tau_-|^p \sin(\Phi_m - \Theta/2) - \mathcal{E}_+ |\tau_+|^p \sin(\Phi_m + \Theta/2)}{\mathcal{E}_0 |\tau_0|^p} \right], \end{aligned} \quad (22)$$

represent the in-phase and in-quadrature components, respectively. Conventional wavelength modulation spectroscopy relies on the assumption that ω_m is small compared to the width of the spectral profile, such that the absorption and phase-shift differences between the various frequency components of the modulation are small. Depending on the nature of the filter, this assumption may become invalid for large p . However, to the extent that this

assumption holds, the output components for a pure FM input field ($\mathcal{E}_- = \mathcal{E}_+$ and $\theta = \pi$) are

$$\begin{aligned}\beta &\approx 2M \frac{|\tau_+|^p - |\tau_-|^p}{|\tau_0|^p} \approx Mp(A_- - A_+) \\ \gamma &\approx 2M\Phi_m.\end{aligned}\tag{23}$$

In this case, β is proportional to the loss difference of the sidebands, and determines the first derivative of the absorption, while γ is proportional to the difference in the phase-shift experienced by the carrier and the average of the phase shifts experienced by the side-bands, and determines the second derivative of the dispersion. Note that $\beta = 0$ for a pure FM output ($\Theta = \pi$). For a pure AM input field ($\mathcal{E}_- = \mathcal{E}_+$ and $\theta = 0$), the components are

$$\begin{aligned}\beta &\approx 2M \frac{|\tau_+|^p + |\tau_-|^p}{|\tau_0|^p} \approx -Mp(A_- + A_+ - 2A_0) \\ \gamma &\approx -M\Theta.\end{aligned}\tag{24}$$

In this case, β is proportional to the difference between the loss of the carrier and the average loss of the sidebands, and determines the second derivative of the absorption, while γ is proportional to the phase difference of the sidebands, and determines the first derivative of the dispersion. Note that $\gamma = 0$ for a pure AM output ($\Theta = 0$).

Eqs. (26) and (24) are the traditional equations for AM/FM spectroscopy. They rely on the assumption that the absorption and dispersion are weak, i.e., there are many modulation cycles per phase shift and each (complex) phase shift is small, $|\Theta - \theta| \ll 2|\omega_m|\tau_c$ and $|A_b| \ll |\alpha|$. In this case, the measured beat-frequency is approximately the modulation frequency, ω_m . On the other hand, this assumption does not hold for large values of $|\tilde{\Theta} - \theta| = p|\tilde{\Phi}_+ - \tilde{\Phi}_*|$. If and there are many complex phase-shifts per modulation cycle, the dispersion can modify the measured instantaneous heterodyne beat frequency, and the absorption can be large enough to alter the shape and size of the modulation ellipse.

3 Sensitivity of the Beat-Note to the Modulation

Notice that the output modulation is phase-shifted with respect to the input by $p(\Phi_+ - \Phi_-)/2$. This phase shift has no effect unless an interferometer or

cavity is present. An interferometer transforms the phase shift into intensity change, whereas a cavity transforms it into a frequency shift. For interferometers, or pulse propagation it is useful to think of the phase shift as modifying spatial frequencies. Provided there is no fluctuation from structure to structure, we may consider the phase shift to be evenly distributed, rather than localized at a particular structure, and replace p with z/L , where z is the propagation distance and L is the length between structures. We can then invoke an effective propagation constant $K = n\omega/c + \Phi/L$. The presence of the resonator structure thus alters the spatial beat-frequency. Comparing the spatial beat-frequencies from Eqs. (17) and (6), we obtain

$$K_b = k_b + K_r, \quad (25)$$

where $K_r \equiv (\Phi_+ - \Phi_-)/2L$ is the contribution to the spatial beat-frequency due to the resonator structure. Hence, the spatial beat-frequency increases for normal dispersion. Any external change in spatial frequency is enhanced by the normal dispersion of the resonator structures, which leads to the conclusion that slow-light can increase the performance of interferometers, whereas fast-light generally decreases their performance (unless its magnitude is quite large).

On the other hand, for cavities it is useful to think of the phase shift as modifying temporal frequencies. If, instead of a sequence of structures, we consider a ring cavity that contains a single structure, then the Q of the cavity will determine the number of passes, p , which becomes infinite for a stable laser cavity. Thus, the effect of a resonator structure in a cavity is considerably larger than in an interferometer. The distance between structures L is set by the cavity length. In this case we replace p wherever it appears with $z/L + t/\tau_c$, where $\tau_c = n_c L/c$ is the round trip time of the cavity. It is assumed that fluctuations in the modulation of Eq. (??) are slower than the cavity round-trip time. We invoke an effective frequency $\Omega = \omega - \Phi/\tau_c$. Again, with each pass, the presence of the resonator structure alters the temporal beat-frequency, and we obtain

$$\Omega_b = \omega_b + \Omega_r, \quad (26)$$

where $\Omega_r \equiv -(\Phi_+ - \Phi_-)/2\tau_c$ is the contribution to the temporal beat-frequency due to the resonator structure. Again, we find that normal dispersion ($\Omega_r > 0$) increases the modulation frequency, i.e., $\Omega_b > \omega_b$, whereas anomalous dispersion ($\Omega_r < 0$) decreases it, i.e., $\Omega_b < \omega_b$, (the sign convention for the phase does not fool us into thinking the opposite). Hence normal

dispersion enhances gyroscopic response. Anomalous dispersion, on the other hand, stabilizes a cavity provided its magnitude is sufficiently small, i.e., for $\Omega_r > -2\omega_b$. The modulation is completely compensated by the coupled resonators when

$$\Omega_r = -\omega_b. \quad (27)$$

which results in perfect cavity self-stabilization, i.e., $\Omega_b = 0$. For anomalous dispersions whose magnitudes are sufficiently large that $\Theta/2 > \omega_m t$, then $\Omega_r < -\omega_b$, and the resulting beat-frequency will be negative. When $\Omega_r < -2\omega_b$, then the magnitude of the resulting negative beat-frequency will be larger than the beat-frequency in the absence of the resonators, i.e., $|\Omega_b| > |\omega_b|$, again resulting in an enhancement of the gyroscopic response.

Note that the phase filter effects any frequency shift that may occur in the cavity. This frequency shift may be due to instability, or it may be a Doppler shift due to rotation of the cavity. The Doppler shift due to rotation can be considered to be simply a strong ($M \gg 1$) AM modulation where the two sidebands represent the two standing-wave eigenmodes, and the carrier frequency results from dissipative effects such as backscattering and/or differential loss. Ideally, for the measurement of rotation, the sidebands will have the same frequencies as the counter-propagating traveling-wave modes, and the residual carrier frequency will be unimportant in comparison with the strong modulation. However, any form of coupling, whether it be conservative (specular reflections) or dissipative (diffuse reflections or differential gain or loss) will cause the sideband frequencies to deviate from the frequencies of the counter-propagating modes, and therefore lead to a reduction in gyro sensitivity at low rates of rotation. Moreover, any dissipative coupling (in the form of back-scattering and/or differential gain or loss) will feed frequencies between the two side modes. If the back-scattering is sufficiently strong, these central frequencies can injection lock the side bands, eliminating the Doppler shift and leading to a dead-band. The amplitude filter effects the relative modulation, and hence the relative size of the dead-band. Therefore, to determine whether a dispersive element improves the performance of a laser gyro, in addition to the modification of the modulation frequency by the dispersion, the modification of the relative modulation by the absorption must also be taken into account.

The interference of the modulation side bands, i.e., of the decaying red- and blue-shifted complex effective frequencies $\tilde{\Omega}_{\pm} = \tilde{\omega}_{\pm} - \tilde{\Phi}_{\pm}/\tau_c$ can be described entirely by a complex effective beat frequency $\tilde{\Omega}_b = -\Delta\tilde{\Phi}_b/2\tau_c =$

$\Omega_b - iA_b/2\tau_c$, that consists of contributions from both the modulation (rotation or instability) and from the (coupled) resonator structure, i.e.,

$$\frac{\tilde{\Omega}_+ - \tilde{\Omega}_-^*}{2} \equiv \tilde{\Omega}_b = \tilde{\omega}_b + \tilde{\Omega}_r \quad (28)$$

where $\tilde{\omega}_b = -\Delta\tilde{\phi}/2\tau_c = \omega_b - i\alpha/2\tau_c = (\tilde{\omega}_+ - \tilde{\omega}_-)/2$ is the gyro beat-frequency in the absence of the (coupled) resonators (i.e., the modulation frequency) and $\tilde{\Omega}_r = -\Delta\tilde{\Phi}_r/2\tau_c = \Omega_r - iA_r/2\tau_c$ is the contribution to the complex beat-frequency from the (coupled) resonators. The beat-note frequency and contrast are represented by the real and imaginary parts of the complex effective beat-frequency

$$\frac{\Omega_+ - \Omega_-}{2} \equiv \Omega_b = \omega_b + \Omega_r \quad (29)$$

$$\frac{A_b}{2\tau_c} = \frac{\alpha + A_r}{2\tau_c} \quad (30)$$

where $\Omega_b = -\Delta\Phi_b/2\tau_c$ is the real-valued effective beat-frequency between the real-valued Doppler-shifted effective frequencies $\Omega_{\pm} = \omega_{\pm} - \Phi_{\pm}/\tau_c$, $\Omega_r = -\Delta\Phi_r/2\tau_c$ is the contribution to the real-valued beat-frequency from the (coupled) resonators, and $A_r = (A_+ + A_-)/2$ is the contribution to the average round-trip loss coefficient from the coupled resonators. Note that each frequency is related to a phase-shift. Hence, Eq. (28) can just as readily be written in terms of phase-shifts

$$\Delta\tilde{\Phi}_b = \Delta\tilde{\phi} + \Delta\tilde{\Phi}_r = \Delta\Phi_b + iA_b \quad (31)$$

where $\Delta\tilde{\phi} = \tilde{\phi}_+ - \tilde{\phi}_-^* = \Delta\phi + i\alpha$ is the complex phase-shift-per-round-trip due to the rotation, and $\Delta\tilde{\Phi}_r \equiv \tilde{\Phi}_+ - \tilde{\Phi}_-^* = \Delta\Phi_r + iA_r$ is the additional complex phase-shift per round-trip due to the (coupled) resonators. The real-valued relation that corresponds to Eq. (31) is $\Delta\Phi_b = \Delta\phi + \Delta\Phi_r$, where $\Delta\phi = \phi_+ - \phi_-$ and $\Delta\Phi_r = \Phi_+ - \Phi_-$.

Note that the quantity $\Delta\tilde{\Phi}_r$ is complex because the resonators act as both a phase and an amplitude filter. Importantly, this additional complex phase-shift depends on $\Delta\phi$, such that both the rotation and the resonators contribute to the total phase-shift per round-trip. If this were not the case, then the sensitivity of the gyro would be unaffected by the presence of the structure (although the beat frequency would be affected). Moreover,

both the real and imaginary parts depend on the rotation, i.e., $\Delta\tilde{\Phi}_r(\Delta\phi) = \Delta\Phi_r(\Delta\phi) + iA_r(\Delta\phi)$. Hence, the gyro sensitivity is determined by the derivative

$$\tilde{\xi} = \frac{d(\Delta\tilde{\Phi}_b)}{d(\Delta\phi)} = \frac{d(\Delta\tilde{\Phi}_b)}{d(\Delta\phi)} - i \frac{d(\Delta\tilde{\Phi}_b)}{d\alpha} = \frac{d(\Delta\tilde{\Phi}_b)}{d(\Delta\phi)} + \frac{dA_b}{d\alpha}. \quad (32)$$

In a laser the saturated gain adjusts itself to maintain a steady-state, i.e., α is a function of A_r , such that the total loss $A_b = \alpha(A_r) + A_r = 0$ stays constant. Hence, $dA_b/d\alpha = 0$, and

$$\tilde{\xi} = 1 + \frac{d(\Delta\tilde{\Phi}_r)}{d(\Delta\phi)} = 1 + \frac{d(\Delta\Phi_r)}{d(\Delta\phi)} + i \frac{dA_r}{d(\Delta\phi)} = \xi' + i\xi'' \quad (33)$$

is a complex enhancement factor whose real and imaginary parts indicate the sensitivity of the beat-note frequency and contrast to the modulation (gyro rotation or cavity instability), respectively.

To determine whether the performance of a gyroscope is improved, we must examine both the real and imaginary parts of ξ . The real and imaginary parts obey the equations

$$\xi' = \frac{d\Omega_b}{d\omega_b} = 1 + \frac{d(\Delta\Phi_r)}{d(\Delta\phi)} \quad (34)$$

$$\xi'' = \frac{d(A_b/2\tau_c)}{d\omega_b} = \frac{dA_r}{d(\Delta\phi)}, \quad (35)$$

i.e., they are slopes that determine the sensitivity of the beat-note frequency and contrast, respectively, to an external modulation. An enhancement in beat-frequency sensitivity occurs provided $|d\Omega_b/d\omega_b| > 1$, i.e., when

$$|\xi'| > 1, \quad (36)$$

Note that this condition can be satisfied for either normal or anomalous dispersion, i.e., the slope can be positive or negative, the only requirement for an enhancement in sensitivity is that its magnitude satisfy Eq. (36). However, whereas normal dispersion (slow light) always enhances gyro sensitivity, anomalous dispersion (fast light) only enhances gyro sensitivity if the magnitude of the dispersion is sufficiently large. Moreover, the beat-note contrast is enhanced when

$$\xi'' < 0, \quad (37)$$

In this case, the side-bands experience less absorption than the carrier frequency, resulting in an increase in the beat-note contrast.

Now, let us recast the derivative in Eq. (33) in terms of the single-pass phase-shift of the resonator structure, rather than that of the cavity. Since $d\phi_c/\tau_c = d\phi_r/\tau_r$, we may make the transformation

$$\begin{aligned} \frac{d(\Delta\tilde{\Phi}_r)}{d(\Delta\phi)} &= \frac{1}{2} \left(\frac{d\tilde{\Phi}_+}{d\phi_+} - \frac{d\tilde{\Phi}_-^*}{d\phi_-} \right) = \frac{1}{2} \left(\frac{d\tilde{\Phi}_+}{d\phi_c} + \frac{d\tilde{\Phi}_-^*}{d\phi_c} \right) \\ &= \frac{1}{2} \left(\frac{\tau_r}{\tau_c} \right) \left(\frac{d\tilde{\Phi}_+}{d\phi_r} + \frac{d\tilde{\Phi}_-^*}{d\phi_r} \right) \\ &= \frac{1}{2} \left(\frac{nl}{n_c L} \right) \left[\left(\frac{d\tilde{\Phi}_+}{d\phi_r} + \frac{d\tilde{\Phi}_-}{d\phi_r} \right) + \frac{i}{2} \left(\frac{dA_+}{d\phi_r} - \frac{dA_-}{d\phi_r} \right) \right] \end{aligned} \quad (38)$$

where $\phi_c = (\omega - \omega_c)\tau_c$ is the single-pass phase-shift in the cavity, $\phi_r = (\omega - \omega_r)\tau_r$ is the single-pass phase-shift in one of the resonators, $\tau_c = n_c L/c$ is the round-trip time in the cavity of length L and refractive index n_c , $\tau_r = nl/c$ is the round-trip time in one of the resonators of length l and refractive index n , and ω_r and ω_c are the resonant frequencies of the resonators and cavity, respectively. Provided the (coupled) resonators are on-resonance with the cavity, i.e., $\omega_r = \omega_c$, then $\tilde{\Phi}_+ = -\tilde{\Phi}_-^*$ ($\Phi_+ = -\Phi_-$ and $A_+ = A_-$), $d\tilde{\Phi}_+/d\phi_c = d\tilde{\Phi}_-^*/d\phi_c$ ($d\tilde{\Phi}_+/d\phi_c = d\tilde{\Phi}_-/d\phi_c$ and $dA_+/d\phi_c = -dA_-/d\phi_c$), and we obtain the more compact expression

$$\frac{d(\Delta\tilde{\Phi}_r)}{d(\Delta\phi)} = \frac{d\tilde{\Phi}_+}{d\phi_c} = \left(\frac{nl}{n_c L} \right) \frac{d\tilde{\Phi}_+}{d\phi_r}. \quad (39)$$

In this case, the enhancement factor can be written

$$\tilde{\xi} = 1 + \frac{nl}{n_c L} \frac{d\tilde{\Phi}_+}{d\phi_r} = 1 + \frac{nl}{n_c L} \left[\frac{d\tilde{\Phi}_+}{d\phi_r} + \frac{i}{2} \frac{dA_+}{d\phi_r} \right] \quad (40)$$

Now, recall that for (coupled) resonator structures $K = n\omega/c + \Phi/L = N\omega/c$ is the effective propagation constant, and N is the effective refractive index. In this case, the distance between structures is equivalent to the cavity size L . The group index is related to the density of such structures per-unit-length, and is defined as

$$\begin{aligned} n'_g \equiv c \frac{dK}{d\omega} &= N + \omega \frac{dN}{d\omega} = n_c + \frac{c}{L} \frac{d\Phi}{d\omega} \\ &= n_c \left[1 + \left(\frac{nl}{n_c L} \right) \frac{d\tilde{\Phi}}{d\phi_r} \right]. \end{aligned} \quad (41)$$

where we have ignored material dispersion. We may also define a complex group index

$$\tilde{n}_g \equiv c \frac{d\tilde{K}}{d\omega} = n_c \left[1 + \left(\frac{nl}{n_c L} \right) \frac{d\tilde{\Phi}}{d\phi_r} \right] = n'_g + i n''_g \quad (42)$$

where $\tilde{K} = n\omega/c + \tilde{\Phi}/L = \tilde{N}\omega/c$ is the complex effective propagation constant, \tilde{N} is the complex effective refractive index, and

$$n''_g = \frac{c}{2\tau_c} \frac{dA}{d\omega} = \frac{1}{2} \left(\frac{nl}{L} \right) \frac{dA}{d\phi_r} \quad (43)$$

is the imaginary part of the group index, which represents the loss dispersion of the structure. The real and imaginary parts of the group index are related by a Kramers-Kronig relation.

For the case when the resonators are on-resonance with the cavity, the relation between the complex group index and complex enhancement factor is readily discerned by comparing Eqs. (40) and (42)

$$\tilde{\xi} = \frac{\tilde{n}_g(\omega_+)}{n_c} = \frac{\tilde{n}_g^*(\omega_-)}{n_c}, \quad (44)$$

Moreover, returning to Eq. (38) we obtain the more general relation for the complex enhancement factor

$$\tilde{\xi} = \frac{\tilde{n}_g(\omega_+) + \tilde{n}_g^*(\omega_-)}{2n_c}. \quad (45)$$

whose real and imaginary parts indicate the effects of the phase and amplitude filters, respectively.

Note that these results are in contrast with those of previous authors who found that the enhancement factor applied to the beat frequency, rather than its sensitivity. In particular, Shahriar et al. correctly predicted that a gyro enhancement could occur for fast light, but incorrectly predicted the magnitude of the enhancement, and found a critical anomalous dispersion (CAD) where the enhancement becomes almost infinite at $n_g = 0$. Instead, we predict the gyro sensitivity to become zero at this point, and that anomalous dispersion only provides an enhancement for $n_g < -n_c$.

In summary, we find that an enhancement in gyro sensitivity occurs when

$$|\xi'| > 1 \text{ and } \xi'' < 0, \quad (46)$$

i.e., the dispersion can be either normal or anomalous, and the relative loss should be higher for the carrier than for the side-band Doppler-shifted frequencies. On the other hand, we find that only anomalous dispersion will self-stabilize a laser cavity. The greatest stability occurs when $n_g = 0$ (CAD) and the range of group indices over which stability occurs is given by

$$-1 < \xi < 1. \text{ and } \xi'' > 0. \quad (47)$$

The stability under CAD conditions appears similar to a dead-band, i.e., the slope of the beat-note vs. rotation (or voltage) becomes zero. However, this is not an injection locking effect. It holds even for a unidirectional laser. We note also, that under CAD conditions a pulse becomes completely spatially extended throughout the fast-light medium. For negative group indices, the pulse is still spatially expanded for indices $n_g > -n_c$, moving backwards in the medium. For indices $n_g < -n_c$, the pulse is actually spatially compressed, similar to what occurs in a slow light medium (but the pulse moves backward). Therefore, an enhanced gyroscopic response is correlated to spatial compression of a pulse, whereas stabilization correlates with spatial expansion. The reason for this is that spatial expansion corresponds to a cavity that is effectively decreased in size, and visa-versa. Again, one of the most interesting cases is $n_g < -n_c$, where the pulse inside the medium is compressed, and moves backwards, but does so slowly (even though it's a fast light medium), thereby corresponding to an increase in the effective cavity size.

4 Analysis of Specific Cases of Interest: Atoms and Resonators

The amplitude and phase filters can work in concert, or against one another for the applications of self-stabilization or gyro enhancement. For atomic media, the amplitude and phase filters work against one another, i.e., decreasing the modulation amplitude increases its frequency and vice-versa, except in one situation: for anomalous dispersions such that $n_g < -1$, the beat frequency is negative, but has a magnitude that is larger than for the case of $n_g = 1$, resulting in an enhanced gyroscopic response.

In the case of two-level atoms, this is clear. For non-inverted two-level atoms, the absorption is higher on-resonance, which attenuates the carrier

frequency more than the sidebands, increasing the relative modulation (index), while at the same time the anomalous dispersion decreases the magnitude of the beat frequency unless $n_g < -1$. If the two-level atom is inverted, the amplification is higher on-resonance, decreasing the relative modulation (index), but now the dispersion is normal, which increases the modulation frequency.

The same is true of coherently prepared three-level atoms. Consider the three prototypical atomic coherence effects of electromagnetically-induced absorption (EIA), electromagnetically-induced transparency (EIT), and gain-assisted superluminality (GAS) from a double-gain line. The case of EIA is similar to an absorbing two-level atom, i.e., absorption accompanied by anomalous dispersion on-resonance increase the relative modulation (index), but decrease the magnitude of the modulation frequency unless $n_g < -1$. For the case of EIT, on the other hand, the transparency and normal dispersion on-resonance result in an increased modulation frequency, but decreased relative modulation (index), i.e., the beat-frequency is enhanced, but so is the relative importance of the dead-band. Finally, in the case of GAS, the higher gain for the sidebands increases the relative modulation (index), but the anomalous dispersion reduces the magnitude of the modulation frequency, except when $n_g < -1$.

Therefore, two-level atoms, EIA, and GAS are useful for gyro enhancement, provided $n_g < -1$. Situations where $n_g > 1$, however, such as EIT and inverted two-level atoms, decrease the relative modulation (index), and thus are not useful for gyro enhancement. Moreover, when $1 > n_g > -1$ the amplitude and phase filters always work against one another, and therefore atomic media are of severely limited use for cavity self-stabilization (stabilization of the frequency is possible but increases the amplitude instability, and vice versa).

The same is not true for optical resonators. The subtle yet important distinction between these materials is that for atomic media the response function, Eq. (9), is Lorentzian, whereas for optical resonators it is an Airy-type expression. A Lorentz medium has poles but not zeros in the complex transmission, whereas resonators have both poles and zeros. The zeros indicate critical coupling, whereas the poles indicate the lasing threshold. Since a Lorentzian medium has no zeros, it cannot possess a critical coupling. Critical coupling corresponds to a reversal in dispersion. It follows that for atomic media the dispersion reverses only when the medium possesses gain, whereas for resonators the dispersion reverses at the critical coupling (even

when it is non-amplifying). Indeed, single under-coupled optical resonators display anomalous dispersion (analogous to a two level atom), whereas single over-coupled resonators display normal dispersion on-resonance, i.e., a reversal from anomalous to normal dispersion occurs at critical coupling. Hence, resonators can be non-amplifying *and* possess normal dispersion (provided they are over-coupled), whereas atoms must be inverted to possess normal dispersion at resonance.

Hence for non-amplifying under-coupled optical resonators, the situation is the same as for atoms, the amplitude and phase filters oppose one another except when $n_g < -1$. For non-amplifying over-coupled resonators, on the other hand, the amplitude and phase filters can work in concert. In this case the on-resonance absorption increases the relative modulation, while the normal (rather than anomalous) dispersion also increases its frequency, which is beneficial for gyro sensitivity enhancement as we have already discussed.

This is emphasized in Fig. (3), where the resonant features of single optical resonators are plotted on an Argand diagram for a variety of couplings. Argand diagrams are a convenient way to plot both the absorption and dispersion of a resonance on the same graph. The complex transmittivity is represented as a parametric phasor, i.e., $\vec{\tau}(\phi) = |\vec{\tau}(\phi)| [\cos \Phi(\phi) \hat{\tau}' + i \sin \Phi(\phi) \hat{\tau}']$. Extremes in transmission occur when $d|\vec{\tau}|/d\phi = 0$ (when $\vec{\tau} \perp d\vec{\tau}/d\phi$), whereas dispersion reversals occur when $d\Phi/d\phi = 0$ (when $\vec{\tau} \parallel d\vec{\tau}/d\phi$, or when the structure is critically-coupled). It will be useful to modify slightly our definition of the complex group index such that we do not need to take the complex conjugate for frequencies below resonance, i.e., we take the derivative of the absorption with respect to $|\phi_r|$ instead of ϕ_r ,

$$n_g'' = \frac{1}{2} \left(\frac{nl}{L} \right) \frac{d\alpha}{d|\phi_r|} = - \left(\frac{nl}{L} \right) \frac{1}{|\tau|} \frac{d|\tau|}{d|\phi_r|}. \quad (48)$$

Hence, both the change in the relative modulation and in the modulation frequency are related to quantities on the Argand diagram, i.e., $d|\tau|/d|\phi_r|$ and $d\Phi/d\phi_r$, respectively. Rewriting, Eqs. (46) and (47) in terms of these quantities

$$\begin{aligned} \frac{d\Phi}{d\phi} > 0 \text{ or } \frac{d\Phi}{d\phi} < -2\frac{n_c L}{nl} \text{ and } \frac{d|\tau|}{d|\phi_r|} > 0 &\Rightarrow \text{Gyro Enhancement} \\ -2\left(\frac{n_c L}{nl}\right) < \frac{d\Phi}{d\phi} < 0 \text{ and } \frac{d|\tau|}{d|\phi_r|} < 0 &\Rightarrow \text{Self-Stabilization} \end{aligned} \quad (49)$$

$$\left\{ \begin{array}{l} -2\frac{n_c L}{nl} > \frac{d\Phi}{d\phi} \text{ or } \frac{d\Phi}{d\phi} > 0 \\ \frac{d|\tau|}{d|\phi_r|} > 0 \end{array} \right\} \Rightarrow \text{Gyro Enhancement} \quad (50)$$

$$\left\{ \begin{array}{l} -2\left(\frac{n_c L}{nl}\right) < \frac{d\Phi}{d\phi} < 0 \\ \frac{d|\tau|}{d|\phi|} < 0 \end{array} \right\} \Rightarrow \text{Self-Stabilization} \quad (51)$$

i.e., whenever $d|\tau|/d|\phi_r|$ and $d\Phi/d\phi_r$ have the same sign, or they are of opposite sign but $d\Phi/d\phi_r < -2n_c L/nl$, then the amplitude and phase filters work together, either enhancing the gyroscopic response or providing cavity self-stabilization. Otherwise, the amplitude and phase filters work against one another. As shown in Fig. (3), there is a dispersion reversal for under-coupled resonators, which prevents both $d\Phi/d\phi > 0$ and $d|\tau|/d\phi > 0$ near $\phi = 0$. Eq. (54) can still be satisfied if the anomalous dispersion is sufficiently large, i.e., $d\Phi/d\phi_r < -2n_c L/nl$. For over-coupled resonators, on the other hand, Eq. (54) is always satisfied.

Coupled resonators can also be of benefit for gyro enhancement. For very weak inter-resonator couplings, the effect of coupled-resonator-induced absorption (CRIA), analogous to EIA can occur. CRIA can be over- or under-coupled, with anomalous or normal dispersion, respectively. Hence, over-coupled CRIA can be used to increase the effect of both the amplitude and phase filters, thus increasing the gyro enhancement even further than a single over-coupled resonator.

However, there is a crucial difference between single resonators and two coupled resonators that is apparent by inspection of Figs. (3) and (4): for single resonators, over-coupling results in slow light at $\phi = 0$, whereas for two coupled resonators, under-coupling results in slow light at $\phi = 0$. Hence, for two coupled resonators, it is only possible to obtain both $d\Phi/d\phi > 0$ and $d|\tau|/d\phi > 0$, i.e., both $\xi' > 1$ and $\xi'' > 1$, for under-coupled CRIA, as shown in Fig. (4).

The enhancement factor depends on the frequency of the sidebands.

When either single or coupled resonators are critically-coupled, the enhancement factor $\xi \rightarrow \infty$ at $\phi_r = 0$. In this case, however, complete absorption of the carrier occurs, and for small rotations the sidebands are also absorbed.

The use of GAS for stabilization would decrease the modulation frequency

but increase the amplitude of the modulation. The use of CRIT (with normal dispersion) to enhance gyroscopic sensitivity would increase the Doppler shift, but attenuate the sidebands, thereby increasing the sensitivity of the system to dissipative processes and concomitantly increasing the dead-band.

For the application of self-stabilization, on the other hand, both the absorption and dispersion must be reversed. However, for optical resonators the dispersion will not reverse again above the lasing threshold, since it already reversed at critical-coupling. Hence, for an amplifying resonator, the gain decreases the modulation, but the normal dispersion increases its frequency, and again the two effects oppose one another. This is generally true for resonators with gain, whether single or coupled they follow the same logic as atoms and are, therefore, of limited use for these applications.

Therefore, the only way to achieve cavity self-stabilization is to use coupled non-amplifying resonators. Coupled-resonator-induced transparency (CRIT) is an effect that occurs in optical resonators and is analogous to EIT. But in contrast to EIT, CRIT may occur with either normal or anomalous dispersion, depending on the coupling between the resonators. (Give the condition here). This is shown in Fig. (5). It is only in this case that the amplitude and phase filters will both demodulate and decrease the frequency of the modulation, leading to complete amplitude and frequency cavity self-stabilization. This is demonstrated in Fig. (6), where the sidebands of an FM modulation are shown with and without the coupled resonator structure.

5 Extra Notes

We assume in this discussion that the splitting of the CW and CCW modes is small in comparison to the splitting that characterizes EIT or CRIT. If the splitting of modes is equal to the CRIT splitting, then, it is here we have the greatest dispersion.

It is also assumed that $\tau_c < 1/\omega_m$, i.e., there are many phase-shifts due to the coupled resonators per modulation cycle. This goes along with the working assumption for a laser gyro, right? If this was not the case, and there were many modulation cycles per round-trip then it would just be a phase-shift. Doesn't this set a fundamental lower limit on the sensitivity of a gyro. Specifically, when the modulation frequency becomes very small, there are few phase shifts per cycle. In this case, the cavity no longer efficiently converts these phase shifts into a change in frequency. Thus, there is a

fundamental lower limit on the sensitivity of a laser gyro.

Also, the sensitivity enhancement should be greater for lower modulation frequencies? The number of phase shifts per cycle is larger in this case, i.e., Ω_r is greater in comparison with ω_b

6 Conclusion

We point out that this is different from resonator-enhanced Sagnac interferometers.

Some numbers

We note, finally, that there exists an analogy between the effects of dispersive and nonlinear elements. Just as the saturation of a laser gain medium compensates intensity variations, a dispersive element can compensate (or enhance) phase variations. Slow-light media increase phase variations, and thus are analogous to saturable absorbers, which increase amplitude noise in lasers. Fast-light media, on the other hand, decrease phase noise, and thus are analogous to two-photon absorbers, which decrease the amplitude noise of a laser.

7 Acknowledgments

The authors acknowledge support from NASA Marshall Space Flight Center Institutional Research and Development Grants CDDF03-17 and CDDF04-08, and the United Negro College Fund Office of Special Programs. This work was supported by the Army Research Office.

8 Appendix A: Another Argument for Self-Stabilization

To understand how self-stabilization can occur, consider the resonant frequencies of the ring cavity, $\omega_q(n_c, L) = 2\pi/\tau_c = q2\pi c/n_c L$, where q is an integer. For stabilization we require that

$$\delta\omega_q = \frac{\delta\omega_q}{\delta L} dL + \frac{\delta\omega_q}{\delta n_c} dn_c \quad (52)$$

$$= -\frac{\omega_q}{L} dL - \frac{\omega_q}{n_c} dn_c = 0 \quad (53)$$

This equation is satisfied when $dL/dn_c = -L/n_c$, i.e., the change in index compensates the change in length. For example, as L increases ω_q decreases, but this may be compensated by a material which decreases n_c thereby increasing ω_q again. Thus, we require a material in which ω_q and n_c change together, i.e., $\delta n_c/\delta\omega_q = n_c/\omega_q$. But an increasing resonance frequency ω_q is equivalent to a decreasing frequency ω , i.e.,

$$\frac{\delta n_c}{\delta\omega} = \frac{\delta n_c}{\delta\omega_q} \frac{\delta\omega_q}{\delta\omega} = -\frac{\delta n_c}{\delta\omega_q} = -\frac{n_c}{\omega_q}. \quad (54)$$

Therefore, it is anomalous dispersion that is required for self-stabilization of a cavity. We further note that some degree of self-stabilization occurs, i.e., the frequency is reduced, when the anomalous dispersion is in the range

$$-2\frac{n_c}{\omega_q} < \frac{\delta n_c}{\delta\omega} < 0. \quad (55)$$

Lower values of $\delta n_c/\delta\omega$ will actually increase the modulation frequency of the instability.

Solving Eq. (41) for the dispersion we obtain

$$\begin{aligned} \omega \frac{dN}{d\omega} &= \frac{c}{L} \frac{d\Phi}{d\omega} - [N - n_c] \\ &= \frac{c}{L} \left[\frac{d\Phi}{d\omega} - \frac{\Phi}{\omega} \right] \approx \left(\frac{nl}{L} \right) \frac{d\Phi}{d\phi}. \end{aligned} \quad (56)$$

Comparing Eqs. (54) and (56) we obtain

$$\frac{d\Phi}{d\phi} = -\frac{n_c L}{nl} \quad (57)$$

This is the anomalous dispersion required to perfectly self-stabilize the cavity. Again, however, some stabilization occurs in the range,

$$-2\frac{n_c L}{nl} < \frac{d\Phi}{d\phi} < 0 \quad (58)$$

which corresponds to group indices $-n_c < n_g < n_c$ or $|n_g| < n_c$.

References

- [1] K. J. Boller, A. Imamoglu, and S. E. Harris, Observation of electromagnetically induced transparency, *Phys. Rev. Lett.*, 66, 2593 (1991).
- [2] G. M. Gehring, A. Schweinsberg, C. Barsi, N. Kostinski, and R. W. Boyd Observation of backward propagation through a medium with a negative group velocity *Science*, 312, 895 (2006).
- [3] U. Leonhardt and P. Piwnitski, Ultrahigh sensitivity of slow-light gyroscope, *Phys. Rev. A*, 62, 055801 (2000).
- [4] A. B. Matsko, A. A. Savchenkov, V. S. Ilchenko, and L. Maleki, Optical gyroscope with whispering gallery mode optical cavities, *Opt. Commun.* 233, 107-112 (2004).
- [5] B. Z. Steinberg, Rotating photonic crystals: A medium for compact optical gyroscopes, *Phys. Rev. E* 71, 056621 (2005).
- [6] J. Scheuer and A. Yariv, Sagnac effect in coupled-resonator slow-light waveguide Structures, *Phys. Rev. Lett.* 96, 053901 (2006).
- [7] Shahriar et al. xxx *Phys. Rev.*
- [8] M. A. Kramer, R. W. Boyd, L. W. Hillman, and C. R. Stroud, Jr., Propagation of modulated optical fields through saturable-absorbing media: A general theory of modulation spectroscopy, *J. Opt. Soc. Am. B* 2, 1444 (1985).
- [9] S. A. Diddams, J. C. Diels, and B. Atherton, Differential intracavity phase spectroscopy and its application to a three-level system in samarium, *J. Opt. Soc. Am. B* 2, 1444 (1985).
- [10] L. Maleki, A. B. Matsko, A. A. Savchenkov, and V. S. Ilchenko, "Tunable delay line with interacting whispering-gallery-mode resonators," *Opt. Lett.* 29, 626-628 (2004).
- [11] J. K. S. Poon, J. Scheuer, Y. Xu, and A. Yariv, "Designing coupled-resonator optical waveguide delay lines," *J. Opt. Soc. Am. B* 21, 1665-1673 (2004).

- [12] M. F. Yanik and S. Fan, "Stopping light all optically," *Phys. Rev. Lett.* 92, 083901(1-4) (2004).
- [13] M. F. Yanik, W. Suh, Z. Wang, and S. Fan, "Stopping light in a waveguide with an all-optical analog of electromagnetically induced transparency," *Phys. Rev. Lett.* 93, 233903 (2004).
- [14] T. Opatrny and D. G. Welsch, "Coupled cavities for enhancing the cross-phase-modulation in electromagnetically induced transparency," *Phys. Rev. A* 64, 23805 (2001).
- [15] D. D. Smith, H. Chang, K. A. Fuller, A. T. Rosenberger, and R. W. Boyd, "Coupled-resonator-induced transparency," *Phys. Rev. A* 69, 63804 (2004).
- [16] H. Chang and D. D. Smith, "Gain-assisted superluminal propagation in coupled optical resonators," *J. Opt. Soc. Am. B* (2005).
- [17] D. D. Smith and H. Chang, "Coherence phenomena in coupled optical resonators" *J. Mod. Opt.* 51, 2503-2513 (2003).
- [18] D. D. Smith, H. Chang, and K. A. Fuller, "Whispering-gallery mode splitting in coupled microresonators," *J. Opt. Soc. Am. B* 20, 1967-1974 (2003).

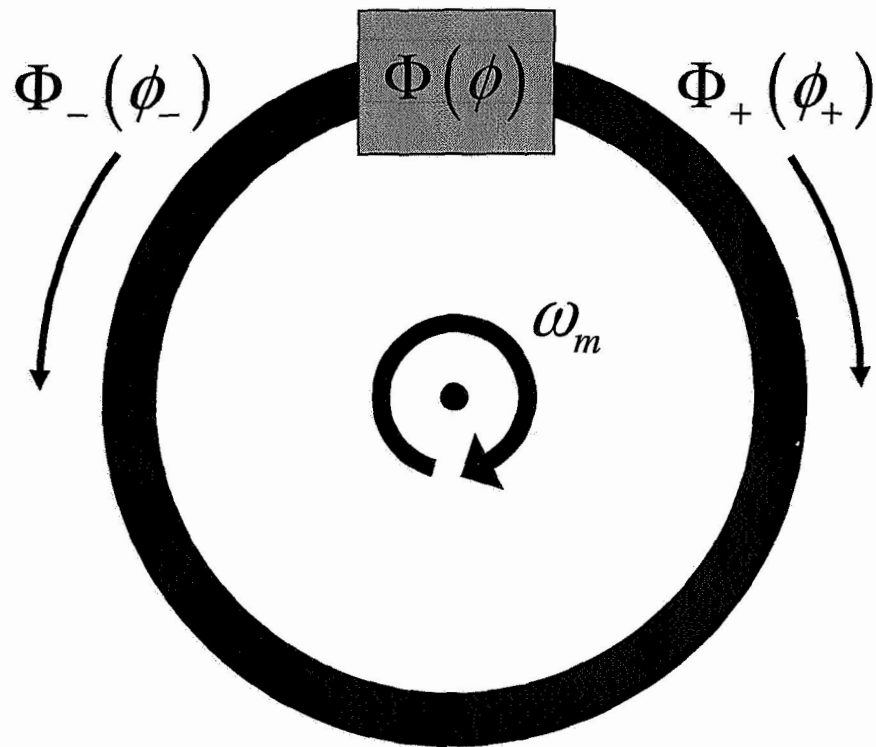


Figure 1: The additional phase-shift Φ due to a dispersive element, represented by the box, is dependent on the phase-shift ϕ due to the modulation (instability or rotation.)

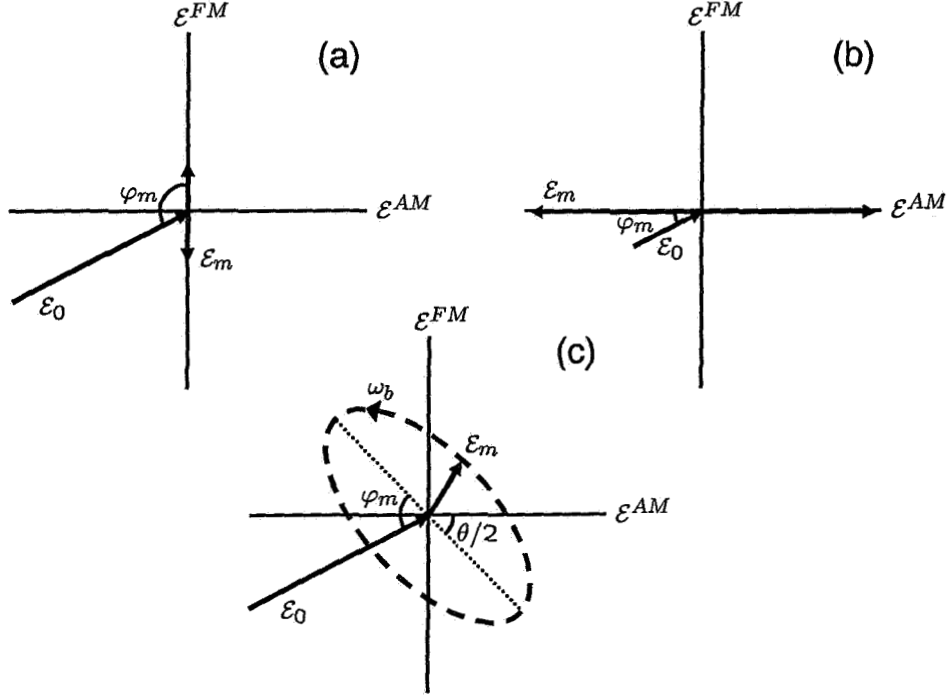


Figure 2: Modulation ellipses for (a) a pure FM ($\theta = \pi$) signal with $M \ll 1$, (b) a pure AM ($\theta = 0$) signal with $M \gg 1$, and (c) a mixed AM/FM signal. The presence of a dispersive element causes the modulation to evolve, in this case from an initially pure AM or FM signal to a mixed signal. In a cavity, the modulation frequency also evolves from ω_m to ω_b provided there are many effective phase-shifts per modulation cycle. The rotation of \mathcal{E}_m can accelerate (gyro enhancement with slow light), decelerate (increased stability), stop completely (perfect stabilization), reverse directions ending up with a decreased speed (increased stability), or reverse directions ending up with an increased speed (gyro enhancement with fast light).

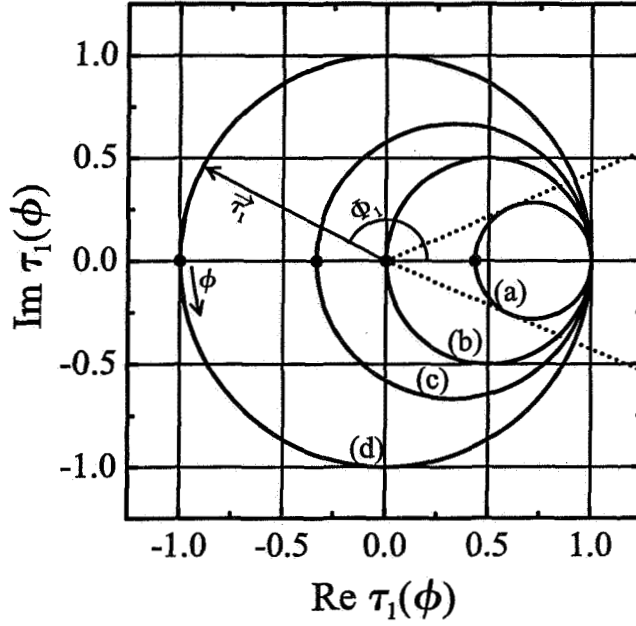


Figure 3: Argand diagram of the complex electric-field transmission for a single resonator: (a) under-coupled, (b) critically-coupled, (c) over-coupled, and (d) over-coupled and lossless. The plots start at the dot $\phi = 0$ and proceed counterclockwise as indicated around the loop over a range of 2π . Dispersion reversals occur when a circle does not contain the origin, and occur at the intersection of the curve with the dotted tangential lines. (The vertical dashed and solid lines indicate $n_g = -1$ and $n_g = \pm\infty$, respectively. Materials whose dispersion circles have origins ($\phi = 0$) to the left of the solid line are over-coupled, which excludes non-inverted two-level atoms. This case is always useful for gyro enhancement since $n_g > 1$. Materials whose dispersion circles have origins to the right of the dashed line cannot be used for gyro enhancement because their anomalous dispersion is too weak, whereas materials whose dispersion circles have origins between the two lines can be used for Gyro enhancement even though they are under-coupled and display anomalous dispersion.)

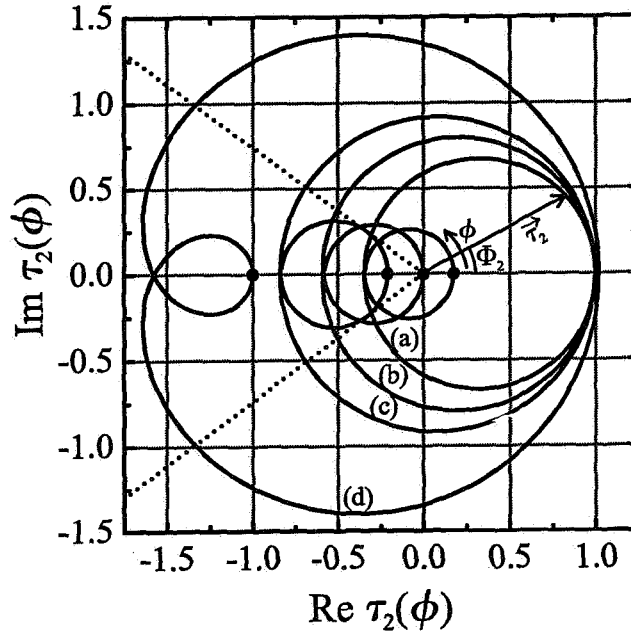


Figure 4: Argand diagram of the complex electric-field transmission for two coupled resonators: (a) under-coupled CRIA ($n_g > 1$ at $\phi = 0$), (b) critically-coupled CRIA ($n_g = \pm\infty$), (c) over-coupled CRIA ($n_g < 1$ at $\phi = 0$), and (d) GAS. (In this case, under-coupled CRIA is always useful for gyro enhancement (this excludes EIA), whereas over-coupled CRIA is useful only when the origin falls between the two vertical lines. For materials (EIA too) (Again, the vertical dashed and solid lines indicate $n_g = -1$ and $n_g = \pm\infty$, respectively.)

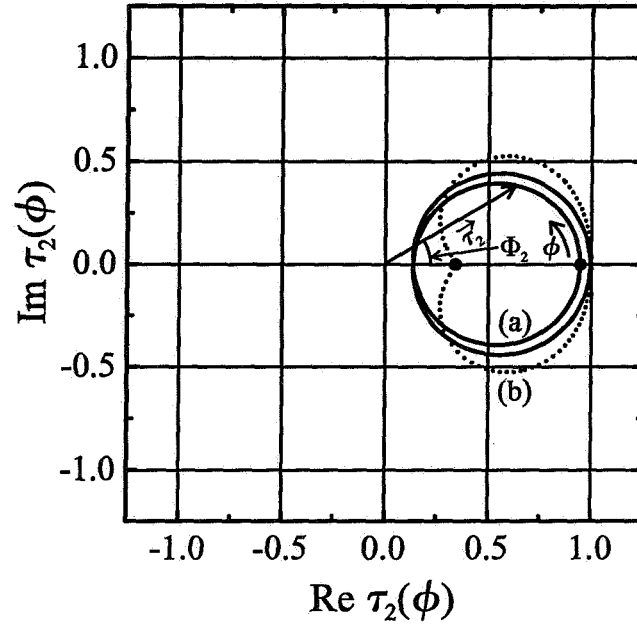


Figure 5: Argand diagram of the complex electric-field transmission for two coupled resonators: CRIT with (a) normal dispersion at $\phi = 0$ and (b) anomalous dispersion at $\phi = 0$. In (b) the inner circle has collapsed to a point, resulting in a cardioid shape and reversing the dispersion. Hence, case (b) is useful for cavity self-stabilization, whereas case (a) is not.

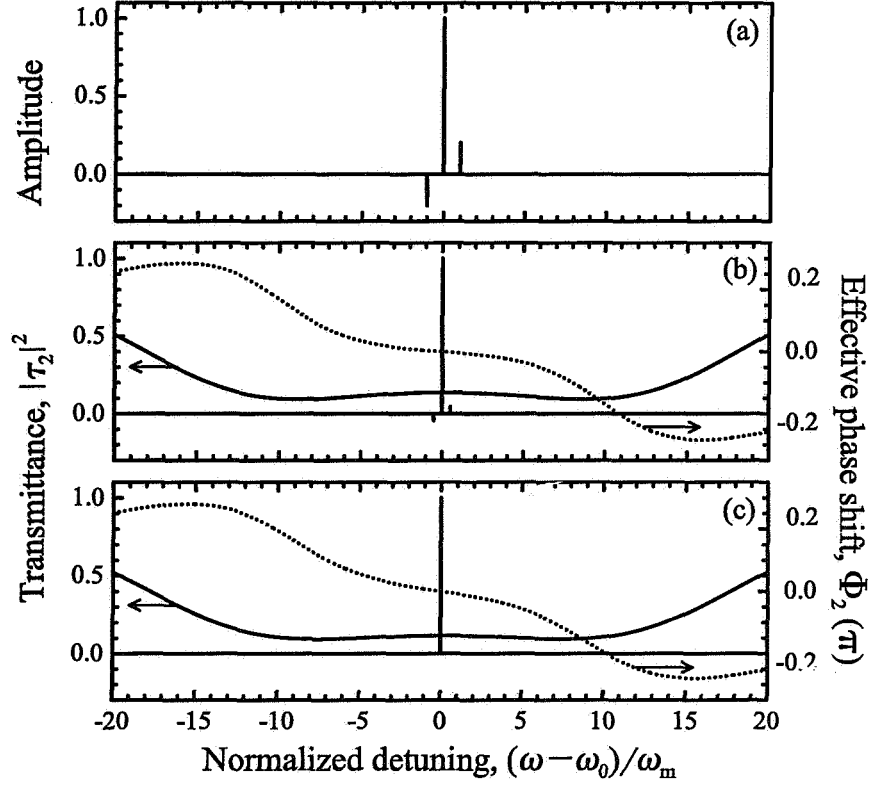


Figure 6: Self-stabilization of a weak FM perturbation applied to a cavity (a) without any resonators ($n_g = 1$, i.e., no self-stabilization) (b) with CRIT in the anomalous dispersion regime ($n_g = 0.5$, i.e., imperfect self-stabilization) and (c) ($n_g = 0$, i.e., perfect self-stabilization). The presence of the resonators decreases both the frequency and relative amplitude of the modulation.

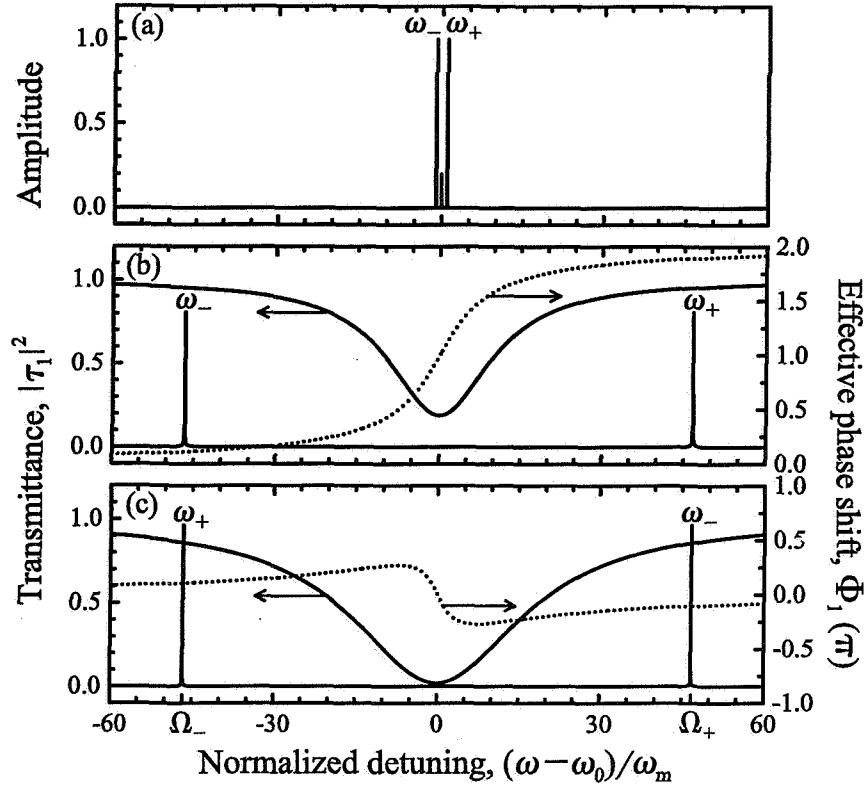


Figure 7: Enhancement of a laser gyro by a single resonator placed within the cavity (a) without the resonator ($n_g = 1$), (b) with an over-coupled resonator ($n_g = 47$) and (c) with an under-coupled resonator ($n_g = -47$). Both the beat-frequency and the relative modulation increase in the presence of the resonators. For case (c), a greater dispersion is required for the same beat-frequency enhancement as in case (b). However, the relative modulation is larger in (c) than in (b). We assume a carrier and modulation frequency of $\omega_0 = 10^{14} Hz$ and $\omega_m = 10 KHz$, respectively, a cavity of $L = 3m$ and $1/\tau_c = 100 MHz$, and a resonator of $Q \approx 10^8$, $1/\tau_r = ?$, and resonance linewidth of about $100 KHz$. (These last numbers for the cavity are not exactly right.)

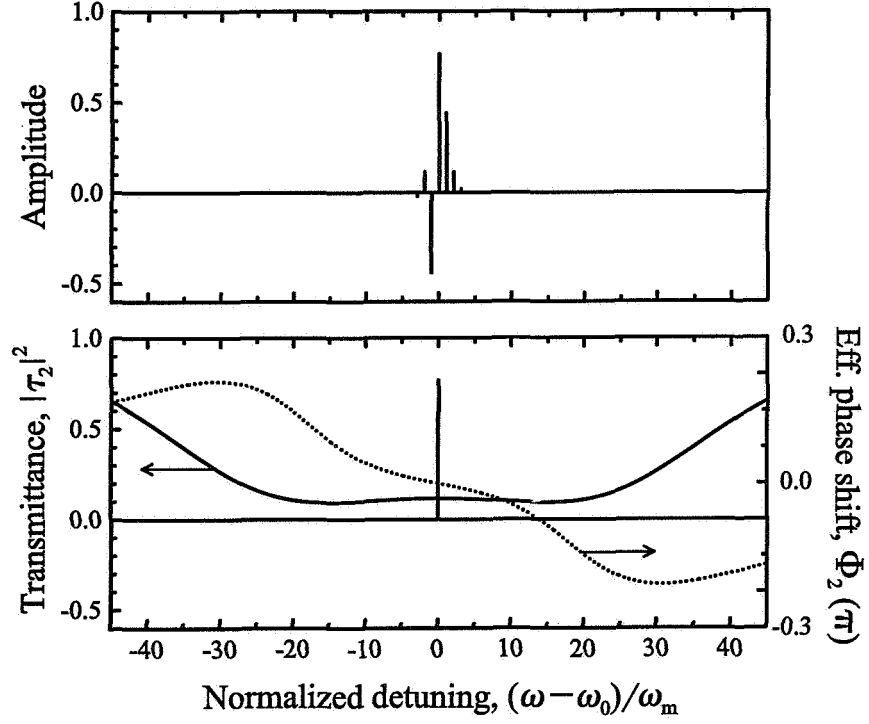


Figure 8: self-stabilization of a strong FM perturbation with multiple sidebands applied to a cavity (a) without any resonators ($n_g = 1$, i.e., no self-stabilization) and (b) $n_g = 0$, i.e., perfect self-stabilization using CRIT in the anomalous dispersion regime.